Molecular Biology of the Cell
Vol. 19, 4918–4929, November 2008

Dynein Light Intermediate Chain: An Essential Subunit That Contributes to Spindle Checkpoint Inactivation

Sarah Mische*, Yungui He*, Lingzhi Ma, Mingang Li, Madeline Serr, and Thomas S. Hays

Department of Genetics, Cell Biology, and Development, University of Minnesota, Minneapolis, MN 55455

Submitted May 15, 2008; Revised August 22, 2008; Accepted September 5, 2008
Monitoring Editor: Kerry S. Bloom

The dynein light intermediate chain (LIC) is a subunit unique to the cytoplasmic form of dynein, but how it contributes to dynein function is not fully understood. Previous work has established that the LIC homodimer binds directly to the dynein heavy chain and may mediate the attachment of dynein to centrosomes and other cargoes. Here, we report our characterization of the LIC in *Drosophila*. Unlike vertebrates, in which two *Lic* genes encode multiple subunit isoforms, the *Drosophila* LIC is encoded by a single gene. We determined that the single LIC polypeptide is phosphorylated, and that different phosphoisoforms can assemble into the dynein motor complex. Our mutational analyses demonstrate that, similar to other dynein subunits, the *Drosophila* LIC is required for zygotic development, germline specification of the oocyte, and mitotic cell division. We show that RNA interference depletion of LIC in *Drosophila* S2 cells does not block the recruitment of a dynein complex to kinetochores, but it does delay inactivation of Mad2 signaling and mitotic progression. Our observations suggest the LIC contributes to a broad range of dynein functions.

INTRODUCTION

There are two families of dynein motor complexes: axonemal dyneins that drive ciliary and flagellar motility, and cytoplasmic dyneins that function in intracellular transport (Vallee *et al*., 2004; Hook and Vallee, 2006). Both are large, multisubunit complexes that share similar structural organization and subunit composition. All dynein complexes include a dimer of heavy chain polypeptides, known to provide the ATPase activity that powers movement along microtubules. The functional roles of the intermediate, light intermediate and light chain polypeptides are less well characterized. Individual subunits, or their variant isoforms, may impart specific functions, such as the attachment of specific cargoes. Consistent with this idea, the intermediate (IC), light intermediate (LIC), and light chain (LC) subunits in vertebrates are encoded by multiple genes that are differentially expressed and alternatively spliced as distinct transcripts in different tissues and cells. In addition, the differential expression and posttranslational modification of subunit isoforms suggests that different combinations of subunits could assemble into distinct complexes (Pfister *et al*., 1996; Tai *et al*., 1998, 2001). This subunit diversity may mediate the interactions of specific binding partners that target and regulate dynein motor activities.

Unlike other dynein subunits, the dynein LIC subunit is unique to cytoplasmic dyneins, suggesting a function specific to intracellular transport. In vertebrates, there are two highly similar *Lic* genes, *DYNC1LI1* and *DYNC1LI2*, which are alternatively spliced and differentially phosphorylated to generate multiple isoforms (Hughes *et al*., 1995; Pfister *et al*., 2006). Several studies have suggested that the LIC subunit is involved in cargo attachment and regulation of dynein-based transport. For example, a direct biochemical interaction between LIC and the core centrosomal protein pericentrin was identified in mammalian cell culture (Purohit *et al*., 1999). The attachment and transport of the pericentrin and γ-tubulin components of centrosomes are reported to depend on dynein (Purohit *et al*., 1999). Similarly, overexpression of Rab4A and LIC-1 in HeLa cells results in the accumulation of both proteins at mitotic centrosomes, evidence that LIC may link the dynein motor to Rab4A on early endosomes (Bielli *et al*., 2001). Consistent with this interpretation, Rab4A interacts directly with LIC-1 in a yeast two-hybrid assay. The *Caenorhabditis elegans* LIC, DLI-1, is required for early embryonic development. RNA interference (RNAi)-mediated depletion of the *DLI-1* transcript in one-cell embryos results in a failure of pronuclear migration, centrosome separation, and centrosome attachment to the pronuclear envelope (Malone *et al*., 2003). Recent work has provided evidence that the hook protein ZYG-12 is associated with the nuclear envelope and recruits dynein, possibly through direct interaction with DLI-1. These results are consistent with earlier studies of dynein heavy chain mutations in *Aspergillus nidulans*, *Neurospora crassa*, *Drosophila*, and *C. elegans* that revealed a role for cytoplasmic dynein in nuclear migration (Plamann *et al*., 1994; Xiang *et al*., 1995; Gonczy *et al*., 1999; Robinson *et al*., 1999).

A third vertebrate *Lic* gene, known variously as *LIC3* (Mikami *et al*., 2002), *D2LIC* (Grissom *et al*., 2002), or *DYNC2LI* (Pfister *et al*., 2006), associates with a less common form of cytoplasmic dynein, Dynein 2. The predominant minus-end motor Dynein 1 (also called cytoplasmic dynein 1a, or DYNC1), functions in a wide range of cellular processes, including organelle and RNA transport, mitotic spindle orientation, and checkpoint signaling (reviewed in Vale,

This article was published online ahead of print in *MBC in Press* (http://www.molbiolcell.org/cgi/doi/10.1091/mbc.E08–05–0483) on September 17, 2008.

* These authors contributed equally to this work.

Address correspondence to: Thomas S. Hays (haysx001@umn.edu).

Abbreviations used: LIC, dynein light intermediate chain.

2003; Vallee *et al*., 2006; Musacchio and Salmon, 2007). Dynein 2 (also called cytoplasmic dynein 1b, or DYNC2) is more restricted in its expression and may function primarily in the assembly of cilia and flagella, including intraflagellar transport (IFT) (Pazour *et al*., 1999; Porter *et al*., 1999; Mikami *et al*., 2002). Dynein 1 and 2 seem to have analogous subunit compositions, but the subunits in each complex are derived from unique genes. Although the third *Lic* gene (*DYNC2LI*) shares some sequence motifs with *DYNC1LI1* and *DYNC1LI2*, the amino acid identity is relatively low (Mikami *et al*., 2002). Putative orthologues have been identified in mammals (Grissom *et al*., 2002; Rana *et al*., 2004), *Chlamydomonas* (Perrone *et al*., 2003), and *C. elegans* (Schafer *et al*., 2003).

Here, we report on the LIC subunit of cytoplasmic dynein 1, or DYNC1, in *Drosophila*. Analysis of LIC function is simplified in *Drosophila* because, unlike vertebrates, the fly Dynein 1 *Lic* is encoded by a single gene. To explore the possible contributions of the LIC subunit to dynein function, we have analyzed loss-of-function mutant phenotypes in whole animals and in germline clones, and we also studied RNAi-induced loss-of-function in S2 tissue culture cells.

MATERIALS AND METHODS

Drosophila Stocks

Fly stocks were obtained from the Bloomington Stock Center (Department of Biology, Indiana University, Bloomington, IN) as listed in FlyBase at www.flybase.org. The *P*-element insertion lines w^{67c23} *P(lacW)*$Dlic^{G0065}$*/FM7c* and w^{67c23} *P(lacW)*$Dlic^{G0190}$*/FM7c* are designated in this text as the alleles $Dlic^{G0065}$ and $Dlic^{G0190}$, respectively. The stock *Df(1)GA112/Dp(1;Y)*y^+v^+*#3/FM7a* was the source of the *Y* chromosome carrying a duplication encompassing the *Dlic* gene. Stocks for germline clone experiments included Bloomington stocks y^1 *w** v^{24} *P(FRT(whs))101* and *w** ovo^{D1} v^{24} *P(FRT(whs))101/C(1)DX*, y^1 f^1*/Y; P(hsFLP)38*, in which the FLP recombination target (FRT) insertion site is located on the *X* chromosome at *14AB*. In some experiments, FLP expression was driven by a *nanos-GAL4, UAS-FLP* chromosome (gift from Corey Goodman, UC Berkeley). Recombinant chromosomes containing the *FRT14AB* insertion and the *Dlic* alleles were generated using standard techniques. *OregonR* was used as a wild-type stock.

Molecular Characterization of the Gene

The Dynein 1 LIC protein sequence from mouse, NM031026, was used with the FlyBase BLAST service to identify the *Drosophila Dlic* gene CG1938. The Dynein 2 LIC protein sequence from *Chlamydomonas*, AAQ12259, was used to identify a *Drosophila* orthologue, CG3769.

For low-stringency Southern blot analysis, fly genomic DNA was hybridized to a ^{32}P-labeled cDNA probe by using standard methods. The expressed sequence tag (EST) clone LD23320, comprising the full length of the *Drosophila* LIC, was used to generate the probe. Final washes were in 2× SSC/0.1% SDS for 3 × 10 min at room temperature, then 3 × 20 min at 42°C.

A genomic clone that includes the *Dlic* transcription unit was isolated from a cosmid genomic DNA library by using the *Dlic* cDNA clone as a probe. An EcoRI/BglII fragment was found to contain the complete *Dlic* gene, including the endogenous promoter and 3′ untranslated region (UTR), and was subcloned into the *P*-element vector *pCaSpeR4* to generate the genomic transgene *P[Dlic$^+$]*.

Genetic Analyses

Mobilization of *P*-element insertions to revert the lethality of $Dlic^{G0065}$ or $Dlic^{G0190}$ was carried out by crossing balanced females, carrying both a *P*-element and the Δ2–3 source of transposase, to males of genotype *Df(1)w67c23*. The absence of the dominant eye shape marker *Bar*, carried on the *FM7c* balancer chromosome, was used to identify candidate male progeny of interest. Excision of the *P*-element was scored by loss of the red-eye marker in Bar^+ males.

Complementation analyses made use of a *Y* chromosomal aberration providing a duplication that includes the *Dlic* gene. Males carrying $Dlic^{G0065}$*/Y-Dp* were crossed to $Dlic^{G0190}$*/FM7c* females to test for complementation of $Dlic^{G0065}$/$Dlic^{G0190}$.

The genomic *Dlic* transgene described above was used to create transgenic lines in a *Df(1)w67c23* background by using standard techniques (Karess and Rubin, 1984). The insertion on the transformant line *P[Dlic$^+$]* used in the work described here was mapped to the second chromosome. Rescue experiments were performed by crossing *P[Dlic$^+$]* males to balanced *Dlic* mutant females, and flies were scored for survival of male progeny carrying the *Dlic* mutation (such males lack the balancer chromosome and therefore have Bar^+ eyes).

The requirement for LIC in oogenesis was examined using the FLP/FRT recombinase system (Golic and Lindquist, 1989; Golic, 1991) and the ovo^{D1}-dominant female sterile mutation (Chou *et al*., 1993; Chou and Perrimon, 1996; Theodosiou and Xu, 1998). *Dlic** mutations were recombined onto chromosomes containing the FRT insertion at *14AB*. Candidate recombinant chromosomes were identified using the mini-white marker associated with the FRT insertion, and the lethality of the *Dlic** mutations. Recombinant chromosomes were confirmed by polymerase chain reaction (PCR) amplification of the FRT sequence, and they were shown to be free of secondary lethal mutations by rescuing the *Dlic** recessive lethal phenotype with *P[Dlic$^+$]*. Germline clones were produced in the presence of ovo^{D1} by crossing balanced *Dlic**, *FRT14AB/FM7c* females to ovo^{D1} males who also contained the *FRT14AB* insertion and expressed the FLP recombinase enzyme under heat-shock control. Eggs were collected for 3–4 d and then larvae were heat-shocked for 1.5 h at 38°C to induce FLP expression. Female progeny expressing *Dlic**, *FRT14AB/*ovo^{D1}, *FRT14AB* were crossed to sibling males and then examined for the presence of developing egg chambers (Table 3). To examine protein distribution and egg chamber morphology, mosaic egg chambers were examined in the absence of ovo^{D1} using males of the genotype *FRT14AB; nanos-GAL4, UAS-FLP* crossed to *Dlic**, *FRT14AB/FM7c* females. Ovaries were prepared for immunofluorescence as described below and probed with the anti-DLIC antibody (described below), monoclonal anti-phosphotyrosine (MP Biomedicals, Irvine, CA), and the nuclear stain ToPro-3 (Invitrogen, Carlsbad, CA) as described below.

Production of Anti-LIC Monoclonal Antibody (mAb) P5F5

A synthetic peptide generated from the *Dlic* cDNA clone LD23320 encoding amino acid residues 378–405 (SPLRSQGVGSNKSGPRTPGTTGQSSPKKIDPK) was used as the antigen in the preparation of hybridoma cell lines and the anti-LIC ascites by the Immunological Resource Center (University of Illinois, Urbana-Champaign, IL).

Protein Methods

Microtubule-associated proteins (MAPs) were prepared from 0 to 20 h *OregonR* embryos as described previously (Hays *et al*., 1994). Briefly, embryos were homogenized on ice in a Dounce homogenizer in 1.5 volumes of PMEG buffer (100 mM piperazine-*N*,*N*′-bis[2-ethanesulfonic acid], pH 6.9, 5 mM MgOAc, 5 mM EGTA, 0.1 mM EDTA, 0.5 mM dithiothreitol, and 0.9 M glycerol) plus protease inhibitors. A 125,000 × *g* extract was prepared, from which dynein was enriched using its ATP-sensitive affinity to Taxol-stabilized microtubules.

Density purification experiments used 2 mg of total protein in soluble extracts of *OregonR* ovaries, embryos, or S2 cells, sedimented through 5–20% sucrose gradients prepared in PMEG buffer, as described in Hays *et al*. (1994). The gradients were centrifuged at 230,000 × *g* for 16 h and collected into 0.5-ml fractions. Sedimentation standards were run in parallel on a separate gradient.

For phosphatase treatment of ovary and embryo extracts, tissues were homogenized in PMEG plus protease inhibitors (described above) and spun for 15 min in a microcentrifuge (~14,000 × *g*). The supernatant was recovered, and 30 μg of total protein was treated with λ-protein phosphatase (New England Biolabs, Ispwich, MA), 30°C for 1 h, in accordance with the manufacturer's instructions. Control reactions included 10 mM each sodium fluoride and sodium orthovanadate as phosphatase inhibitors.

Immunoprecipitation from ovary extracts was carried out as described in Boylan *et al*. (2000)). Briefly, monoclonal antibodies were first allowed to bind protein A-Sepharose beads (Sigma-Aldrich, St. Louis, MO), and then incubated with equal amounts of ovary extract (0.6 mg of total protein) for 3 h at 4°C. After washing, each pellet was eluted into 15 μl of 2× SDS-polyacrylamide gel electrophoresis (PAGE) sample buffer, and the entire volume was loaded onto a gel for blot analysis.

SDS-PAGE was performed on 7.5% (or 5–17% gradient) minigels, which were then transferred to polyvinylidene difluoride membrane (Millipore, Billerica, MA). Blots were probed with anti-LIC monoclonal P5F5 (1:3000), anti-DHC monoclonal P1H4 (1:10,000; McGrail and Hays, 1997), anti-IC MAB1618 (1:2500; Millipore Bioscience Research Reagents, Temecula, CA), anti-Tctex-1 polyclonal 1246 (1:1000; Li *et al*., 2004), or anti-actin monoclonal JLA20 (1:1000; Developmental Studies Hybridoma Bank, University of Iowa, Iowa City, IA). Proteins were detected using alkaline phosphatase-linked secondary antibodies with the Tropix chemiluminescence system (Applied Biosystems, Foster City, CA) or, as in Figure 2A, with the chromogenic substrate nitro blue tetrazolium/5-bromo-4-chloro-3-indolyl phosphate (Sigma-Aldrich).

Densitometry measurements were performed using ImageJ (National Institutes of Health, Bethesda, MD) on immunoblots of samples loaded onto the same gel, and processed as described above; immunoblots were cut horizontally to detect each protein independently. Film exposures used for quantification were below saturation, as established by multiple exposures. Images were digitized with a Canoscan 9950F (Canon U.S.A., Lake Success, NY). Protein expression levels were normalized to that of actin, which was used as the loading control.

S2 Cell Culture, Chemical Treatments, and RNA Interference

Drosophila S2 cells were cultured in M3 insect medium (Sigma-Aldrich) supplemented with 10% insect medium supplement (Sigma-Aldrich) plus 2% fetal bovine serum and penicillin/streptomycin. Transfections were performed as described previously (Han, 1996). Cells were plated on concanavalin A-treated coverslips (Rogers *et al*., 2002).

For colchicine treatment, S2 cells were allowed to attach to coverslips for 30–60 min, and then they were treated with 1 μg/ml colcemid (Sigma-Aldrich) for 4 h before fixation. Treatment with MG132 (Sigma-Aldrich) used a concentration of 10 μM at room temperature for 2 h, before plating on treated coverslips.

For RNAi, cells were treated with 2 μg of double-stranded (ds)RNA for 4 d. PCR templates for dsRNA were generated from *Drosophila* EST clone LD23320. Control and RNAi-treated S2 cells were plated onto concanavalin A-treated slides for 1 h before fixation (Rogers *et al*., 2002). dsRNAs were prepared by in vitro transcription using the MegaScript T7 kit (Ambion, Austin, TX) according to the manufacturer's instructions, using the following primers: *Dlic*: forward 5′-t7-GTC GGC GAT ATT GAA TGA-3′, reverse 5′-t7-CGT CGA TCG AGT TGT TG-3′; *Dhc*: forward 5′-t7-CGC GAG TCG CCA GAG GTG-3′, reverse 5′-t7-CGG AAC TTG CGC ATG TGC TC-3′; *Dic*: forward 5′-t7-ACT TGG CCC GCC AGA G-3′, reverse 5′-t7-CAT CGC CGT TTC CGC C-3′; and *Tctex-1*: forward 5′-t7-CTT TGC TTT CCG CAT CCC-3′, reverse 5′-t7-TTC ATC GCG AAT TCC GGC-3′

For reverse transcription (RT)-quantitative (q)PCR, total RNA from S2 cells was prepared using TRIzol Reagent (Invitrogen) and subsequently treated with DNase. First-strand cDNA was generated using Invitrogen SuperScript II First Strand Synthesis System for RT-PCR, and quantitative PCR was performed in a Stratagene Mx3000P cycle using Platinum SYBR Green qPCR SuperMix (Invitrogen). The mRNA was quantified by normalizing to a glyceraldehyde-3-phosphate dehydrogenase (GAPDH) control template. Primers used for amplification were as follows: *GAPDH*: forward 5′-AATTAAGGCCAAGGTTCAGGA-3′, reverse 5′-ACCAAGAGATCAGCTTCACGA-3′; *Dhc:* forward 5′-CTGTCATTGATGCGCAAGCAG-3′, reverse 5′-GTTATGTTCTCTGTACCGAAG-3′; *Dic:* forward 5′-GCCGAACAACGAGTAAAGAC-3′, reverse 5′-GCCTCCTCCATGTCCTTGATC-3′; *Dlic:* forward 5′-GAATTCATGGCGATGAACAGTGGGAC-3′, reverse 5′-CTCGACGCCCTGCAGTTTGGC-3′; and *TCTEX-1*: forward 5′-GATGGATGACTCACGCGAAG-3′, reverse 5′-GTCCAGCACCGTTCTTTTGC-3′.

Immunofluorescence Microscopy

Ovaries were dissected from 2- to 3-d-old *OregonR* females, and then they were fixed and stained as described previously (McGrail and Hays, 1997). Embryos aged 0–3 h were fixed as described in Hays *et al.* (1994). Identical antibody dilutions were used for the immunofluorescent staining of ovaries and embryos. Anti-LIC antibody P5F5 was diluted 1:50, anti-phosphotyrosine antibody (MP Biomedicals) diluted 1:50, and ToPro-3 iodide anti-DNA dye (Invitrogen) diluted 1:2000. Secondary antibodies conjugated to Alexa 488 and Alexa 568 (Invitrogen) were diluted 1:200.

S2 cells were fixed and stained essentially as described in (Maiato *et al*., 2006), with minor modifications. Fixation was 10 min in 4% paraformaldehyde in cytoskeleton buffer (137 mM NaCl, 5 mM KCl, 1.1 mM Na_2HPO_4, 0.4 mM KH_2PO_4, 2 mM MgCl, 2 mM EGTA, 5 mM PIPES, and 5.5 mM glucose, pH 6.9). Primary antibody incubations were carried out in blocking buffer (10% fetal bovine serum in phosphate-buffered saline-Triton [PBS-T] [PBS with 0.1% Triton X-100]) for 1 h in 37°C, and secondary antibody incubations for 1 h at room temperature, with three 5-min washes in PBS-T after each incubation. Antibody dilutions were as follows: anti-dynein heavy chain (DHC) P1H4 (1:600), anti-tubulin DM1A-fluorescein isothiocyanate conjugate (1:1000; Sigma-Aldrich), anti-phospho-histone H3 (1:1000; Millipore), anti-centromere identifier (CID) (1:2400; Henikoff *et al*., 2000), and anti-Mad2 (1:40; Logarinho *et al*., 2004). Secondary antibodies conjugated to Alexa 488 and Alexa 568 (Invitrogen) or Cy5 (GE Healthcare, Little Chalfont, Buckinghamshire, United Kingdom) were diluted 1:600.

All specimens were examined on a Nikon Eclipse TE200 inverted microscope equipped with the PerkinElmer Confocal Imaging System (PerkinElmer Life and Analytical Sciences, Boston, MA). Egg chambers were imaged with a 60× 1.4 plan-apochromat lens. Embryos and S2 cells were imaged with a 100× 1.4 plan-apochromat lens.

Kinetochore fluorescence intensity was quantified from image stacks by using a method based on (King *et al*., 2000; Hoffman *et al*., 2001). Total pixel brightness was measured for a small rectangular area centered over a single kinetochore. Kinetochore location was determined by visualizing CID staining in a separate channel. Background fluorescence per unit area was calculated for a region framing each rectangle, then scaled to the area of the rectangle and subtracted from the initial total brightness measurement. The resulting number was considered to be the corrected signal. The statistical mean and SD were determined from measurements of at least 15 kinetochores, scoring one to two kinetochores per cell for each treatment condition. Statistical analyses used two-tailed *t* tests; $p < 0.05$ is significant.

RESULTS

Identification of the LIC in Drosophila

To understand the function of the LIC subunit of cytoplasmic dynein, we began by examining the gene in *Drosophila*. Fly genome sequence database analyses map the *Dlic* gene to the region 10A8 on the X chromosome and predicts eight exons spanning 8.8 kb (Figure 1A; see also FlyBase). Our Southern blot experiments using a *Dlic* cDNA probe under low-stringency conditions confirm that the LIC subunit is encoded by a single gene (Figure 1B). FlyBase lists four different EST clones for the *Drosophila Dlic*, three of which are ubiquitously expressed and differ only in short segments within the 5′ UTR. They are predicted to encode a single protein of 493 residues with molecular weight of ~55 kDa. The fourth EST, represented by only a single clone, is transcribed from the second intron and is predicted to produce a truncated protein lacking the N-terminal 95 residues. Our Northern blot experiments failed to detect the smaller transcript (data not shown), and the functional relevance of this truncated LIC is unknown. Using a *Chlamydomonas* LIC3 protein sequence to BLAST search the *Drosophila* genome, we also identified a putative orthologue of the vertebrate Dynein 2 *Dlic* gene CG3769 (previously reported by Grissom *et al*. 2002). Comparison of the predicted Dynein 1 and Dynein 2 *Drosophila* LIC sequences reveals only a low level of homology (19% amino acid identity; Figure 1C). The work reported here will focus on the LIC subunit of Dynein 1, the predominant cytoplasmic dynein in *Drosophila*.

To study the distribution of the LIC subunit, we generated a mAb, P5F5, which specifically recognizes the Dynein 1 LIC (see *Materials and Methods*; Figure 1C). Immunoblot analysis of *Drosophila* ovary and embryo extracts using the mAb reveals an LIC protein doublet of ~55/57 kDa (Figure 2A). In other organisms, the LIC is modified by phosphorylation (Gill *et al*., 1994; Hughes *et al*., 1995). Treatment with λ protein phosphatase enzyme reduces the *Drosophila* LIC doublet to a single, smaller protein, consistent with the interpretation that the slower migrating LIC isoform is phosphorylated (Figure 2A). Both phosphoisoforms are present in dynein prepared by microtubule affinity (Figure 2B), and both cosediment on sucrose density gradients with the dynein heavy and IC subunits in a 19S particle (Figure 2C). We do not observe LIC in fractions other than the 19S peak, suggesting there is not a significant pool of polypeptide outside the dynein complex. Immunoprecipitation experiments using the anti-LIC mAb also recover the dynein complex (Figure 2D). These results demonstrate that the LIC is an integral subunit of the dynein motor complex.

Dlic Is Essential for Drosophila Development

To address LIC function, we conducted a mutational analysis, using two fly strains containing separate *P*-element insertions within the LIC genomic region. Both lines are recessive larval lethal and fail to complement each other for viability, suggesting that they are allelic. Inverse PCR and sequence analysis of the flanking regions confirmed the positions of both *P*-elements within the Dlic. The $Dlic^{G0065}$ insertion falls within the first intron at nucleotide 382, and the $Dlic^{G0190}$ insertion is found in the splice donor site in the seventh intron. Neither insertion disrupts a second gene, CG32668, located within the first intron of Dlic (Figure 1A).

We demonstrated that the observed lethality was specifically due to *P*-element disruption of the *Dlic* gene and not to a second-site lethal mutation. First, mobilization of the *P*-elements in both fly lines generated precise excisions that reversed the lethal phenotypes (Table 1). In addition, we

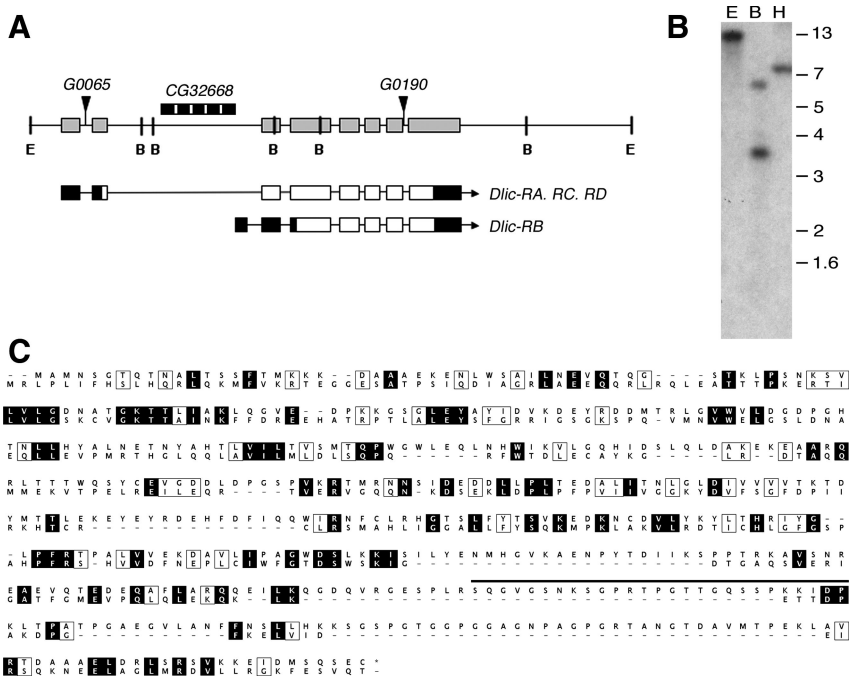

Figure 1. A single gene encodes the Dynein1 *Dlic* in *Drosophila*. (A) Schematic shows order of introns (thin bars) and exons (wide bars) of *Dlic* genomic region. Positions of the *P*-element insertions are designated by triangles. An unrelated gene, CG32668 (hatched bar), lies within the second intron of *Dlic*. FlyBase identifies four potential ESTs for *Dlic*; CG1938-RA, -RC, and -RD correspond to the full-length DLIC protein sequence, and CG1938-RB is proposed to result from alternative splicing and use of an alternative start site, generating a shorter protein. We were unable to detect the shorter transcript. Predicted coding regions of the transcripts are indicated by open bars; noncoding regions by black bars. The relative locations of restriction enzyme sites in the *Dlic* genomic region are shown: E, EcoRI, B, BamHI. (B) A Southern blot of wild-type *Drosophila* DNA digested with EcoRI (E), BamHI (B), or HindIII (H) was hybridized with radiolabeled *Dlic* cDNA. Identical results were obtained under conditions of high or low stringency. All bands recognized correspond to sizes predicted from the sequence of the *Dlic* gene. (C) Alignment of the predicted peptide sequences of LIC subunits for Dynein 1 (top) and Dynein 2 (below). Identical residues are in shaded boxes, similar residues in open boxes, and gaps are indicated by dashes. The location of the peptide used for antigen production is shown by a bar (—) positioned over the Dynein 1 LIC sequence.

rescued the lethality of both *P*-element insertions with a full-length *Dlic* genomic transgene (see *Materials and Methods*). Thus, we conclude that the *Dlic* is an essential gene, and the *P[Dlic$^+$]* transgene characterized in these studies is fully functional (Table 2).

Dynein Accumulation and Function during Oogenesis Requires LIC

To examine which dynein functions are mediated by the LIC, we characterized its distribution in egg chambers. In wild-type ovaries, 16-cell egg chambers are formed in the germaria when cystoblasts undergo four mitotic divisions. Incomplete cytokinesis results in structures called ring canals, which allow for the transfer of cytoplasmic factors between the cells. Ultimately, one of the 16 cells differentiates as the oocyte, whereas the remaining cells function as nurse cells to support oocyte development (Spradling, 1993). We previously showed that the dynein heavy chain (HC) and IC (IC) subunits accumulate early in the presumptive oocyte, and by midoogeneisis become concentrated at the oocyte posterior (McGrail and Hays, 1997; Boylan *et al*., 2000; Li *et al*., 2004). Our cytological analysis of LIC shows a pattern of localization that is indistinguishable from that of dynein HC and IC (Figure 3A).

To further examine the role of LIC in oogenesis, we used the FLP/FRT system with the dominant female sterile *ovoD* mutation (see *Materials and Methods*). By generating homozygous mutant clones within heterozygous females, this technique allows the study of mutations that would otherwise be lethal. The FLP/FRT system induces site-specific mitotic recombination, and the *ovoD* mutation allows identification of recombination events in the germline. (Because *ovoD* prevents development beyond early oogenesis, any eggs produced must result from recombination events leading to the loss of *ovoD* and the concomitant generation of homozygous *Dlic* mutant clones.)

Ovaries from females expressing lethal *Dlic* mutations in the germline were scored for maturing egg chambers. Of the 488 ovaries examined, only 1% showed late stage egg chambers (Table 3). This result suggests that the mutant LIC does not support oogenesis. In control experiments carried out in the presence of the *P[Dlic$^+$]* transgene, 82% (n = 250) of the ovaries contained maturing egg chambers. The ability of *P[Dlic$^+$]* to rescue the production of normal egg chambers demonstrates that LIC, like other dynein subunits, is required for proper female germline development.

Moreover, the germline phenotypes of mutant *Dlic* clones are identical to those caused by clones of dynein heavy chain mutations (McGrail and Hays, 1997). To facilitate closer cytological examination of the mutant egg chambers, we repeated the *Dlic* mosaic analysis using a wild-type background instead of the *ovoD* mutation. *Dlic* mutant germline clones were distinguished from wild-type clones by the absence of LIC protein detected by the monoclonal anti-LIC antibody. Additionally, the egg chambers were double-labeled with a DNA dye to examine the cell number and size of the nuclei (Figure 3, B and C). In wild-type egg chambers, LIC protein accumulates to the oocyte, and there is a com-

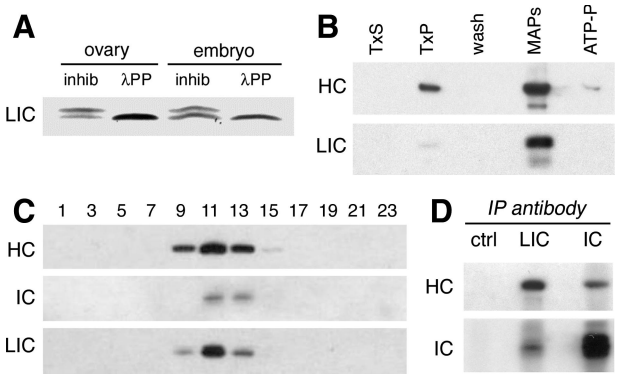

Figure 2. The LIC is phosphorylated and copurifies with other dynein subunits. (A) An immunoblot of wild-type ovary and embryo extracts probed with the anti-LIC mAb P5F5 identifies a protein doublet with mobility of ~55/57 kDa. Treatment with λ protein phosphatase (λPP) reduces the doublet to a single band. Phosphatase inhibitors (inhib) were included in the control reaction. Identical results are obtained when the starting material is partially purified dynein. This blot was developed using a chromogenic substrate, to facilitate resolution of the protein bands. (B) Preparation of microtubule-associated proteins from embryos. Like other dynein subunits, the LIC is enriched in the microtubule pellet (TxP) and is released from microtubules in the presence of ATP. Equal total protein is loaded in each lane. TxS and TxP: supernatant and pellet after stabilization of microtubules by Taxol. MAPs and ATP-P, supernatant and pellet after elution with ATP. The blot was probed with antibodies against dynein HC and LIC. The doublet of LIC isoforms is not resolved by the 7.5% PAGE gel, and in this blot the lower band recognized by the anti-LIC antibody is likely to be a proteolytic fragment. (C) Sucrose density gradient fractionation of ovary extracts reveals the cosedimentation of LIC with the dynein HC and dynein IC in a peak corresponding to ~19S. Equal volumes of alternate fractions are loaded in each lane. (D) Antibodies against the LIC coimmunoprecipitate both the dynein HC and dynein IC subunits from ovary lysate. No dynein is seen in the beads/no antibody control (ctrl).

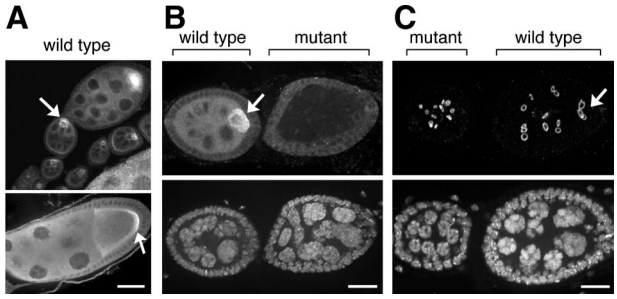

Figure 3. Immunolocalization of LIC in *Drosophila* ovaries. (A) In wild-type ovaries, LIC becomes enriched in the oocyte (arrows), similar to other dynein subunits. By stage 9 (bottom), LIC is concentrated at the posterior of the oocyte in a pattern similar to the heavy chain and IC subunits. Bar, 20 μm (applies to both panels). (B and C) In germline clones of *Dlic* mutations, the oocyte fails to develop and cell division is disrupted. Egg chambers were probed to identify LIC by using the LIC-specific antibody (B, top), DNA (B and C, bottom), or ring canals (C, top). In wild-type egg chambers, the oocyte (arrow) is identified by the accumulation of DLIC (B), a diploid nucleus, and the four ring canals adjacent to the oocyte (C). By contrast, the *Dlic* mutant egg chambers fail to differentiate an oocyte, lack DLIC (B), contain only polyploid nuclei, and show a disorganized pattern of ring canals (C). Bars, 5 μm.

plete set of 16 germline cells per egg chamber, consisting of 15 polyploid nurse cells and one diploid oocyte (Figure 3B, arrow). In contrast, *Dlic* mutant egg chambers fail to accumulate LIC signal in the germline, and all germline cells contain polyploid nuclei (Figure 3, B and C, mutant), indicating the diploid oocyte was never specified. We used an antibody against a phosphotyrosine epitope present in the ring canals to study the pattern of cell cleavage within the egg chambers. In wild-type egg chambers, four ring canals are positioned adjacent to the oocyte (Figure 3C, arrow), but the *Dlic* mutant egg chambers show a disorganized pattern of ring canals (Figure 3C, mutant). This indicates an aberrant pattern of cell cleavage that likely results from improper spindle orientation or fusome morphogenesis during formation of the egg chamber (McGrail and Hays, 1997; de Cuevas

Table 1. Reversion of lethality by precise excision of P-element insertions in the *Dlic* gene

		Progeny			
Maternal genotype	Paternal genotype	*Dlic*[a]*/Revertant*	*Dlic*/Y*	*FM7*/Revertant*	*FM7/Y*
Dlic1/FM7	Revertant1/Y	**136**[b]	0	142	98
Dlic2/FM7	Revertant2/Y	**133**	0	138	106

[a] Asterisks (*) indicates the presence of the listed allele, or corresponding revertant chromosome.

[b] Female progeny with a *Dlic* mutation and revertant chromosome are the class of interest (numbers in bold).

Table 2. Rescue of *Dlic* lethal mutations by the genomic transgene *P*[*Dlic*$^+$]

Allele	*Dlic*/+ +/*CyO*	*Dlic*[a]/+ *P*[*Dlic*+]/+	*FM7*/+ +/*CyO*	*FM7*/+ *P*[*Dlic*+]/+	*FM7/Y*+ /*CyO*	*FM7/Y* *P*[*Dlic*+]/+	*Dlic*/Y*+ /*CyO*	*Dlic*/Y* *P*[*Dlic*+]/+
Dlic1	129	126	113	132	86	92	0	**88**[b]
Dlic2	123	133	116	144	88	89	0	**97**

[a] Asterisks (*) indicates the presence of the *Dlic* mutation listed in the left column.

[b] Males with a balanced copy of the *Dlic* transgene *P*[*Dlic*$^+$] on the second chromosome were crossed to females containing the *Dlic** mutation balanced over the *FM7c* chromosome. Males with the *Dlic** mutation and *P*[*Dlic*$^+$] are the class of interest (numbers in bold).

Table 3. Mosaic egg chambers lacking *Dlic* fail to develop

Genotype	No. of females analyzed	No. of ovaries with eggs/total number of ovaries
Dlic/P[ovo^D]*	244	4/488
Dlic/P[ovo^D]; P[Dlic+]*	125	205/250

Site-specific recombination was induced between homologous chromosomes carrying the *Dlic** mutation and the female sterile mutation *ovoD* (see *Materials and Methods*). In the presence of the *ovo^D mutation, Dlic* mutant ovaries show a nearly complete loss of mature egg chambers. In control experiments, development is rescued by the *P[Dlic+]* transgene.

and Spradling, 1998). Two thirds of the egg chambers had fewer than the normal 16 cells, further evidence of a role for the LIC in cell division (Table 4). We also examined the distribution of dynein HC in *Dlic* mosaic egg chambers. The heavy chain protein was not enriched in a single cell and instead was evenly distributed throughout the whole egg chamber (Supplemental Figure 1). These results suggest that LIC is required for all known dynein functions during formation of the oocyte.

RNAi Depletion of LIC in S2 Cells Delays Mitotic Progression

The abnormal cleavage patterns and decreased cell numbers observed in *Dlic* mosaic egg chambers suggest a role for LIC in mitosis. This is consistent with previous work localizing dynein to mitotic spindle structures, and the mitotic defects resulting from the loss of other dynein subunits (Hays *et al*., 1994; Echeverri *et al*., 1996; Merdes *et al*., 1996; Robinson *et al*., 1999; Wojcik *et al*., 2001; Maiato *et al*., 2004; Griffis *et al*., 2007; Yang *et al*., 2007). To investigate LIC function in mitotic cell division, we used RNAi to reduce LIC protein levels in *Drosophila* S2 cultured cells. LIC depletion over a 5-d period of dsRNA treatment was monitored by quantitative immunoblot analysis. As early as the second day of treatment, the level of LIC is reduced by more than one-third, and after 4 d of treatment only a minor amount of LIC is detected (Figure 4A). The RNAi depletion of LIC also significantly reduces, but does not eliminate, the protein levels of dynein HC and IC subunits. On average less than one fifth of HC, and approximately one third of the IC, remain after 4 d of *Dlic* dsRNA treatment. In contrast, the level of the 14-kDa Tctex-1 light chain subunit is relatively stable under the same conditions. The decrease in other dynein subunits after *Dlic* RNAi suggests that the LIC is required for stability of the dynein complex. Our quantitative PCR indicates that although *Dlic* mRNA is greatly decreased by the RNAi treatment, mRNA expression of other dynein subunits is not (Figure 4B). We also conducted reciprocal experiments to monitor the stability of different subunits after RNAi depletion of the HC, IC or Tctex-1 light chain. As with *Dlic* RNAi, reduction of HC or IC results in a similar loss of other subunits, with the exception of Tctex-1 (Figure 4C). Consistent with its nonessential role (Li *et al*., 2004), levels of Tctex-1 do not decrease after depletion of other subunits, nor does its depletion affect the levels of other subunits. Together, these results suggest that the HC, IC, and LIC polypeptides are more stable when incorporated into the dynein complex.

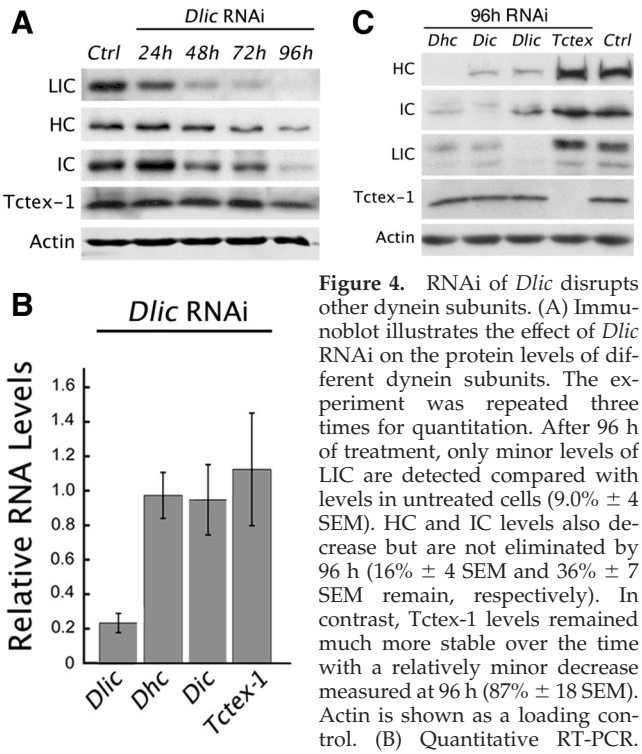

Figure 4. RNAi of *Dlic* disrupts other dynein subunits. (A) Immunoblot illustrates the effect of *Dlic* RNAi on the protein levels of different dynein subunits. The experiment was repeated three times for quantitation. After 96 h of treatment, only minor levels of LIC are detected compared with levels in untreated cells (9.0% ± 4 SEM). HC and IC levels also decrease but are not eliminated by 96 h (16% ± 4 SEM and 36% ± 7 SEM remain, respectively). In contrast, Tctex-1 levels remained much more stable over the time with a relatively minor decrease measured at 96 h (87% ± 18 SEM). Actin is shown as a loading control. (B) Quantitative RT-PCR. Graph depicts changes in levels of RNA transcripts for different dynein subunits following *Dlic* RNAi treatment. Transcript levels are normalized to the corresponding levels observed in the absence of RNAi treatment. Only *Dlic* shows a significant ($p < 0.001$) reduction in RNA expression. The changes in protein expression observed for other dynein subunits (shown in A) are not paralleled by corresponding reductions in levels of RNA transcripts. Error bars show ± SEM; n = 4 experiments. (C) Protein blot summarizes how RNAi depletion of different subunits alters protein levels of other subunits. Tctex-1 is unaffected by the loss of other subunits.

Table 4. Abnormal frequencies of germline cell divisions in *Dlic* mutant egg chambers

	Maternal genotype	
No. of germline cells/ egg chamber	*Dlic*, FRT; FLP/ +*(n = 33)[a]	*Dlic*, FRT; FLP/P[Dlic+]*(n = 27)[b]
16	11	27
14	12	0
12	3	0
10	1	0
8	5	0
6	1	0
4	1	0
2	1	0

To evaluate whether *Dlic* is involved in the mitotic divisions of early oogenesis, germline clone experiments were conducted in a wild-type background (see *Materials and Methods*). Egg chambers were stained with the LIC antibody and double-labeled with a nuclear stain to allow nuclei to be counted. We counted the total number of germline cells in *Dlic** mosaic egg chambers and in mosaic egg chambers rescued by the *P[Dlic$^+$]* transgene. A majority of the *Dlic** mosaic egg chambers have fewer than the normal 16 germline cells.

[a] Full maternal genotype: *Dlic*, FRT/FRT; nanos-Gal4, UAS-FLP/+*.

[b] Full maternal genotype: *Dlic*, FRT/FRT; nanos-Gal4, UAS-FLP/P[Dlic+]*.

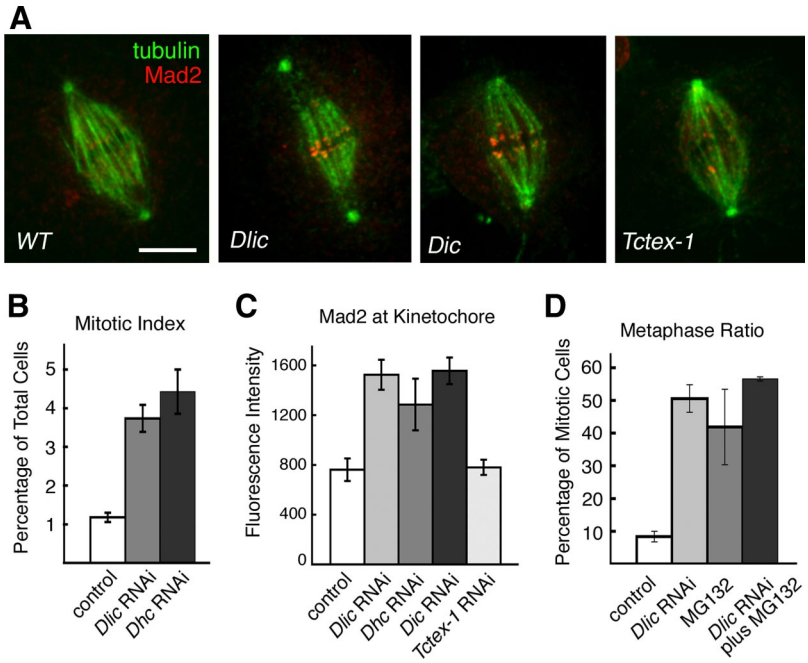

Figure 5. Depletion of LIC by RNAi disrupts mitotic progression. (A) Immunolocalization of tubulin (green) and Mad2 (red) in metaphase S2 cells. In wild-type cells (WT), the spindle assembly checkpoint protein Mad2 localizes transiently to kinetochores early in mitosis, but its kinetochore accumulation is lost or greatly reduced by metaphase (Logarinho *et al*., 2004; Buffin *et al*., 2005; Griffis *et al*., 2007). Depletion of dynein by RNAi of *Dlic*, *Dic*, or (data not shown) *Dhc* prevents release of Mad2. Note the detached centrosomes, typical of spindle morphology defects after loss of dynein. Consistent with results in Figure 4C, spindle structure and Mad2 staining after RNAi depletion of Tctex-1 seem indistinguishable from wild type. Bar, 5 μm. (B) The loss of LIC after RNAi, like loss of the dynein HC, significantly increases the mitotic index (percentage of cells in mitosis). Fixed cells were scored visually using antibody staining of the histone H3 phosphoprotein. Graph shows mean $\pm$ SEM; n = four independent experiments, at least 2000 cells counted per experiment. (C) Quantitation of kinetochore Mad2 fluorescence after RNAi, as illustrated in A. Total pixel fluorescence intensity at aligned kinetochores was measured in fixed cells. A significant increase in Mad2 intensity results from RNAi of *Dlic*, *Dhc*, and *Dic*, but not *Tctex-1*. The number of cells examined for each condition ranged from 17 to 40. See also Supplemental Table 1. (D) Consistent with the Mad2 accumulation, we find that *Dlic* RNAi causes a significant increase in the metaphase ratio (percentage of mitotic cells in metaphase). Treatment with both RNAi and the anaphase inhibitor MG132 does not decrease the metaphase ratio compared with MG132 alone ($p > 0.05$), from which we infer LIC depletion does not significantly interfere with prometaphase congression of chromosomes and their alignment at the metaphase plate.

We find that the RNAi depletion of LIC disrupts checkpoint signaling and the progression of mitosis. Similar to results following the loss of dynein heavy chain function (Wojcik *et al*., 2001; Griffis *et al*., 2007), *Dlic* RNAi treatment causes a fourfold increase in the mitotic index of S2 cell cultures (Figure 5). In addition, the checkpoint signaling protein, Mad2, displays an abnormal accumulation at the kinetochores of metaphase chromosomes (Figure 5, A and C, and Supplemental Table 1). Changes in Mad2 levels were evaluated by comparing the fluorescence intensities at aligned kinetochores in RNAi-treated and control cells (see *Materials and Methods*). Kinetochore accumulation of Mad2 is observed after RNAi depletion of the HC and IC subunits as well, but not after depletion of the Tctex-1 light chain. Here again, Tctex-1 is distinct from other dynein subunits; it is apparently not required for dynein function in checkpoint signaling. Previous studies in *Drosophila* embryos and S2 cells have also implicated dynein heavy chain function in centrosome migration, spindle pole attachment, and chromosome movement during mitosis (Robinson *et al*., 1999; Savoian *et al*., 2000; Wojcik *et al*., 2001; Maiato *et al*., 2004; Griffis *et al*., 2007; Yang *et al*., 2007). We find that detachment of centrosomes and loss of spindle pole convergence are common defects in *Dlic* RNAi-treated *Drosophila* cells. However, despite abnormalities in spindle morphology, chromosomes still align at the metaphase plate (see Figures 5A and 6A). Depletion of LIC increases the frequency of metaphase in mitotic cells approximately fivefold over control cells (Figure 5D; $p < 0.01$), suggesting that LIC is required for the transition from metaphase to anaphase. To measure whether loss of LIC function also affects chromosome movements during prometaphase, we looked at the percentage of cells that accumulate at metaphase in the presence of the chemical anaphase inhibitor MG132 (Maia *et al*., 2007). If the absence of LIC causes defects in prometaphase, we would expect to see fewer cells reach metaphase following treatment with both RNAi and MG132, than with MG132 alone. Instead, we find that the percentage of mitotic cells arrested at metaphase is similar under either condition (Figure 5D). Our observations suggest that LIC depletion does not block the alignment of chromosomes at the metaphase plate but does interfere with removal of the Mad2 checkpoint protein from kinetochores and the initiation of anaphase.

Dynein Transit off Kinetochores Depends on the LIC Subunit

Previous studies provide evidence that dynein actively moves off kinetochores and along kinetochore microtubules during chromosome congression (Howell *et al*., 2001; Wojcik *et al*., 2001). Moreover, the similar transport of checkpoint proteins off the kinetochore depends on dynein function. In *Drosophila*, mutations that disrupt dynein HC function block the shedding of both kinetochore dynein and the Rod checkpoint protein (Wojcik *et al*., 2001). The accumulation of the

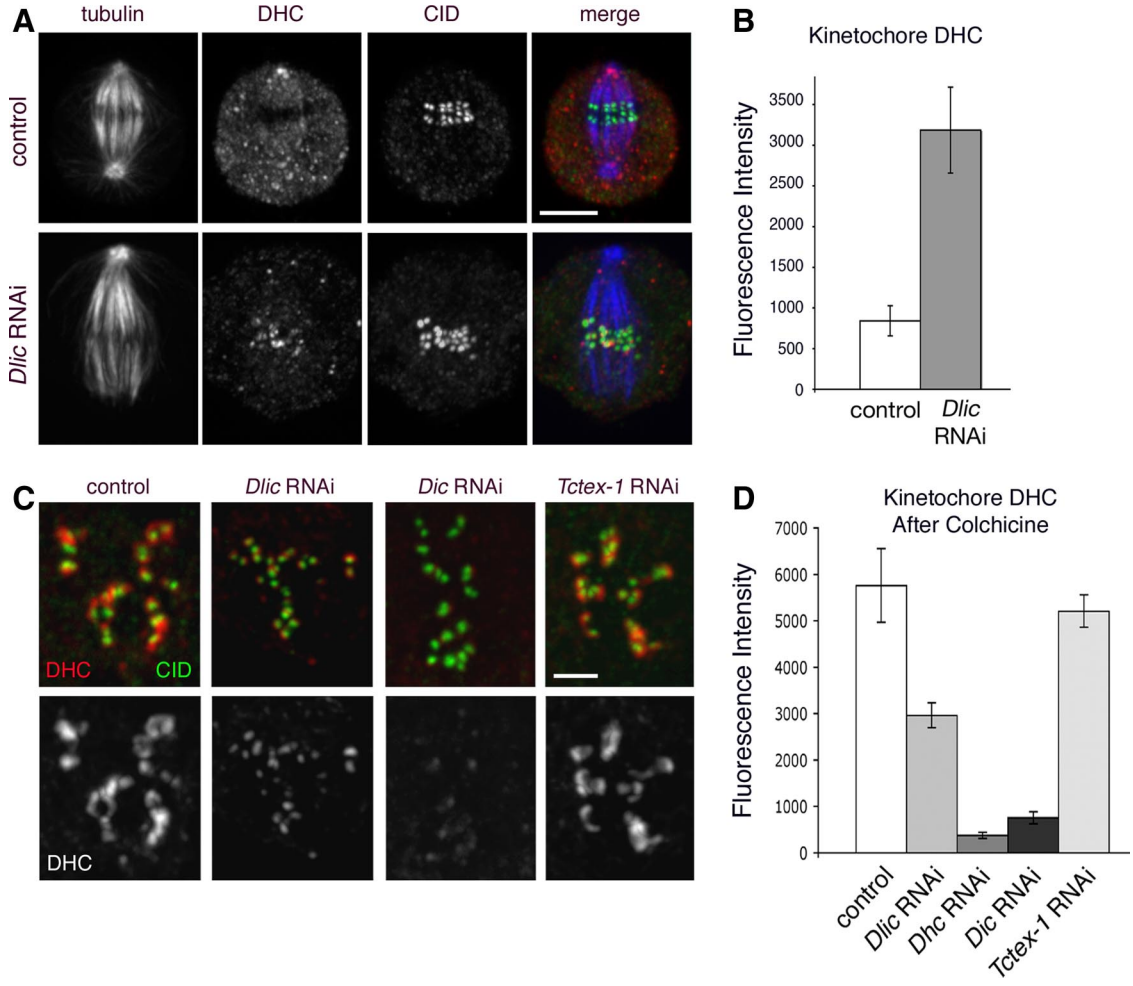

Figure 6. LIC is required for dynein to move off the kinetochore but not to bind the kinetochore. (A) Immunolocalization of dynein (DHC; red) and CID, a kinetochore marker (green), in metaphase S2 cells. In untreated control cells, dynein is present along the spindle and throughout the cytoplasm but is distinctly decreased in the region of the metaphase plate. After *Dlic* RNAi, dynein is enriched at kinetochores. Bar, 5 μm. (B) The intensity of the dynein HC signal at metaphase kinetochores was determined after *Dlic* RNAi (see *Materials and Methods*). Error bars indicate ± SEM. See also Supplemental Table 2. (C) Cells were treated with colcemid to remove kinetochore microtubules, thereby preventing dynein from exiting the kinetochore. Under these conditions, cells depleted of LIC still show some dynein accumulation at kinetochores. In contrast, in the absence of IC, binding of dynein HC to kinetohcores is largely suppressed. Bar, 2 μm. (D) Quantitation of experiments illustrated in C. Bar graph shows mean relative intensity of DHC, ± SEM. For each condition, n = 31–39 kinetochores. See also Supplemental Table 3.

checkpoint protein Mad2 at kinetochores after RNAi depletion of LIC (Figure 5) suggests that dynein motor activity and transit off kinetochores is dependent on LIC. To further examine this hypothesis, we quantitated the changes in dynein accumulation at aligned metaphase kinetochores in control and *Dlic* RNAi-treated cells (Figure 6, A and B, and Supplemental Table 2). To facilitate this analysis, we treated cells with MG132 for 2 h to enrich for metaphase cells containing aligned chromosomes (Orr *et al*., 2007). Consistent with previous reports (Wojcik *et al*., 2001), in wild-type *Drosophila* cells, dynein streams off kinetochores and along kinetochore microtubules toward the spindle poles (Supplemental Movie 1). Kinetochore dynein is progressively depleted during prometaphase until it is no longer detectable at the kinetochores of aligned metaphase chromosomes (Figure 6A). If LIC is required for dynein activity and transport off the kinetochore, then *Dlic* RNAi should block the loss of kinetochore dynein. Consistent with this prediction, we find that dynein HC and IC polypeptides accumulate at aligned metaphase kinetochores after LIC RNAi treatment (Figure 6A). The fact that the dynein is retained at the kinetochore suggests that it is nonfunctional, indicating successful depletion of the LIC subunit. In addition, LIC depletion reduces tension on sister kinetochores, despite normal microtubule density associated with the kinetochores (Supplemental Figure 2). Our results are similar to those reported for the disruption of mitotic dynein/dynactin function in mammalian cells (Yao *et al*., 2000; McEwen *et al*., 2001; Howell *et al*., 2001; Stehman *et al*., 2007). Together, our results support the interpretation that Mad2 removal requires dynein motor activity in addition to microtubule attachment.

Our visualization of HC and IC at kinetochores following LIC depletion also implies that the attachment of the dynein motor to kinetochores does not require the LIC subunit. To examine this more closely, we exploited the fact that dynein accumulates to high levels at kinetochores following colcemid treatment and the consequent loss of kinetochore microtubules (Howell *et al*., 2001; Wojcik *et al*., 2001; Basto *et al*., 2004). We quantitated changes in dynein accumulation at unattached kinetochores when the colcemid treatment fol-

lowed RNAi depletion of different dynein subunits (Figure 6, C and D). In the case of cells treated with colcemid alone, the levels of dynein HC, as well as IC (data not shown), were substantially elevated (Figure 6, C and D, and Supplemental Table 3). When cells are exposed to both *Dlic* RNAi and colcemid treatments, dynein HC still accumulates at kinetochores, albeit to a lesser extent than in the presence of colcemid alone. This result is corroborated when the experiment is repeated using a LIC-GFP construct to visualize LIC at the kinetochore (Supplemental Figure 3). By comparison, RNAi depletion of IC significantly reduces levels of dynein HC at kinetochores even after colcemid treatment. Dynein HC accumulation after depletion of the Tctex-1 subunit is similar to the wild-type control (Figure 6, C and D). Based on these results we propose that the LIC is not required for dynein binding to unattached kinetochores.

DISCUSSION

We present here a functional characterization of the *Drosophila* LIC of Dynein 1 (also called *Dlic2*; see FlyBase). Using *Dlic* mutant alleles and RNAi, we find that LIC function is required for *Drosophila* egg chamber development and oocyte specification, as well as for regulation of checkpoint signaling in mitotic S2 cells. Our results provide evidence that the LIC subunit is critical for dynein stability and activity.

The LIC null phenotypes reported here are similar to the phenotypes for strong loss-of-function mutations in other core dynein subunits in *Drosophila*, as well as in other organisms and cells (Dick *et al*., 1996; Gaglio *et al*., 1997; Harada *et al*., 1998; Gonczy *et al*., 1999; Robinson *et al*., 1999; Boylan and Hays, 2002; Gaetz and Kapoor, 2004; Maiato *et al*., 2004; Pfister *et al*., 2006; O'Rourke *et al*., 2007). One explanation for the similarity in phenotypes is that the assembly of core dynein subunits, including the HC, IC, and LIC, is an interdependent process. We find that depletion of the LIC subunit by RNAi results in the destabilization of the dynein complex and the IC and HC polypeptides. In reciprocal experiments, when either the IC or HC are eliminated by RNAi, the core dynein subunits and assembled complex exhibit a similar reduction in stability. The interdependent assembly of core dynein subunits is also consistent with the lack of free subunits outside the dynein complex. Together, these results suggest that partially assembled subcomplexes, or free, soluble, core dynein subunits are less stable than complete complexes and are ultimately degraded.

Previous studies concerning the stability of dynein subunits and subcomplexes are few, with apparently conflicting results. Consistent with our in vivo data, in vitro observations using salt-dissociated vertebrate extracts show that a HC/LIC dynein subcomplex is unstable. Moreover, the dynein subcomplex can be stabilized in reconstitution experiments with the IC and LC polypeptides (King *et al*., 2002). In contrast, experiments in yeast indicate that the core dynein subunits do not exhibit interdependent stability. The expression of dynein HC/Dyn1 in budding yeast is reportedly unchanged in the null LIC/Dyn3 mutant background, although HC/Dyn1 function and cortical dynamics are inhibited. In addition, the IC/Pac11 and LIC/Dyn3 polypeptides are present at wild-type levels in the Dyn1Δ mutant. The discrepancy between these results and our own could reflect a bona fide difference in the regulation of dynein stability in lower eukaryotes, or instead, may reflect an increased stability of the epitope-tagged subunits that were monitored in the yeast experiments (Lee *et al*., 2005).

Unlike the interdependence of HC, IC, and LIC stability, our results demonstrate that stability of the accessory Tctex-1 light chain is independent of the other core dynein subunits. The elimination of Tctex-1 by RNAi has no effect on HC, IC, and LIC stability; and conversely, RNAi depletion of HC, IC, or LIC has little, if any, effect on the stability of Tctex-1 (Figure 4C). These observations are consistent with our previous finding that Tctex-1 is the only nonessential dynein subunit in *Drosophila* (Li *et al*., 2004). Our experiments do not address the contribution of the LC8 and LC7 light chain subunits to dynein stability. However, based on their essential functions (Dick *et al*., 1996; Bowman *et al*., 1999) and previously reported evidence for their role in dynein assembly and stability (DiBella *et al*., 2004; Nikulina *et al*., 2004), it seems likely that the stability of the LC7 and LC8 light chains is dependent on the other core dynein subunits. Our analysis leaves open the possibility that the essential core subunits may also mediate interactions with specific binding partners and contribute to the specialization of dynein function. To reveal such specialized functions for individual subunits, it will be important to identify alleles that support dynein assembly, but disrupt specific functional subdomains within the subunits.

The full repertoire of dynein function during mitosis continues to be debated, but there is growing support for its role in checkpoint inactivation at kinetochores (reviewed in Musacchio and Salmon, 2007; Burke and Stukenberg, 2008). Spindle assembly checkpoint proteins are recruited to unattached and/or unaligned kinetochores, where their activation and release are thought to generate the diffusible signal that blocks the anaphase-promoting complex, thereby delaying anaphase onset. Previous experiments have established that dynein also accumulates at kinetochores before chromosome attachment and congression to the metaphase plate (Pfarr *et al*., 1990; Steuer *et al*., 1990; Echeverri *et al*., 1996; King *et al*., 2000). Moreover, we and others have shown that removal of dynein and checkpoint proteins from kinetochores is dependent on dynein motor activity and the attachment of kinetochore microtubules (Howell *et al*., 2001; Wojcik *et al*., 2001; Basto *et al*., 2004; Griffis *et al*., 2007). During prometaphase, kinetochore dynein actively walks off the kinetochore and along the associated microtubules, carrying away checkpoint proteins, including Mad2 and Rod. Significantly, mutations and/or inhibitors that compromise dynein motor function, or pharmacological treatments that eliminate kinetochore microtubules, result in accumulation of kinetochore dynein and checkpoint proteins to high levels (Howell *et al*., 2001; Wojcik *et al*., 2001; Basto *et al*., 2004). In the present study, we extend these observations to show that movement of dynein off kinetochores and along kinetochore microtubules is inhibited by the RNAi depletion of the LIC subunit. Our results suggest the LIC is required for dynein motor activity and the silencing of checkpoint signaling. In the absence of LIC, both dynein HC and the spindle checkpoint protein Mad2 accumulate at the kinetochores of aligned metaphase chromosomes, and the mitotic index is significantly elevated. This is in marked contrast to the substantial depletion of dynein from aligned metaphase kinetochores in untreated control cells containing the full complement of dynein subunits.

There are multiple ways that dynein might contribute to the inactivation of checkpoint signaling. Blocking any of these dynein activities would maintain checkpoint signaling and delay mitotic progression. As suggested previously, dynein could remove Mad2 sites from the kinetochore (Howell *et al*., 2001) or similarly could remove Zw10 and Rod from the kinetochore (Wojcik *et al*., 2001; Kops *et al*., 2005). Alternatively, dynein could contribute to silencing the checkpoint by producing tension at kinetochores. Disrup-

tion of kinetochore dynein could directly reduce tension at kinetochores as a consequence of defective microtubule attachment and reduced force production. Alternatively, the inhibition of dynein function could indirectly reduce tension at kinetochores by severing spindle pole attachment and the anchorage of kinetochore fibers.

A simple interpretation of recent observations is that dynein acts directly to remove checkpoint components from the kinetochore. First, there is considerable evidence that checkpoint signaling is activated at unattached kinetochores. Checkpoint proteins and dynein accumulate at unattached kinetochores in mitosis and are depleted upon microtubule attachment and biorientation (reviewed in Musacchio and Salmon, 2007; Burke and Stukenberg, 2008). In addition, we showed previously that the Rod checkpoint protein physically associates with dynein and dynactin (Basto *et al*., 2004); and colocalizes with dynein in both wild-type and mutant dynein backgrounds (Wojcik *et al*., 2001). Blocking motor activity with a dynein mutation blocks the depletion of both dynein and Rod from the kinetochore. These results suggest the motor activity of kinetochore dynein directly determines the localization of the associated Rod checkpoint protein. Moreover, studies that target the specific disruption of kinetochore dynein also support dynein-dependent transport of Mad2 (Howell *et al*., 2001; Griffis *et al*., 2007; Stehman *et al*., 2007).

Tension alone does not seem to regulate the removal of Rod and Mad2 from kinetochores. Taxol is known to reduce kinetochore tension but does not affect kinetochore microtubule number or removal of Mad2 (Yao *et al*., 2000; McEwen *et al*., 2001). In the presence of Taxol, the Rod checkpoint protein also continues to be actively transported off kinetochores and along the attached microtubules (Basto *et al*., 2004). In contrast, although tension is also reduced following LIC RNAi, both dynein and Mad2 are retained at kinetochores. We do not see a significant decrease in kinetochore microtubules, similar to results following dynein inhibition in mammalian cells (Howell *et al*., 2001). Although dynein plays a role in the microtubule attachment in the initial stages of prometaphase (Yang *et al*., 2007), these results suggest that at later stages of chromosome congression, the kinetochore microtubule attachment does not apparently depend on dynein. Moreover, microtubule attachment, though necessary, is not sufficient for checkpoint protein removal. We favor the interpretation that LIC depletion inactivates the dynein motor and blocks the microtubule-dependent transport of dynein and associated checkpoint proteins off the kinetochore (Howell *et al*., 2001; Wojcik *et al*., 2001; Kops *et al*., 2005; Musacchio and Salmon, 2007; Stehman *et al*., 2007; Burke and Stukenberg, 2008). Whether additional dynein activities elsewhere within the spindle also contribute to tension and checkpoint regulation requires further investigation.

The binding of dynein to mitotic kinetochores is complex, involving a number of direct and indirect interactions, including associations with the checkpoint complex Rod-Zw10-Zwilch (Starr *et al*., 1998; Williams *et al*., 2003), the dynactin complex (Echeverri *et al*., 1996; Tai *et al*., 2002), Lis1 (Faulkner *et al*., 2000), Spindly (Griffis *et al*., 2007), and Nudel (Liang *et al*., 2007). Less well studied are how individual dynein subunits act to mediate these associations. Significantly, we find the dynein HC and IC accumulate on unattached kinetochores in the presence of colcemid after LIC depletion. Thus, the loss of LIC does not seem to block the binding of dynein to unattached kinetochores. However, the accumulation of dynein after LIC depletion is somewhat reduced compared with treatment with colcemid alone. We interpret this to reflect the lowered stability of the dynein complex resulting from the depletion of LIC. Because the LIC binds to the HC at a site just C-terminal to the IC binding site (Tynan *et al*., 2000), we suggest that LIC may mediate changes in HC conformation that in turn modulate interactions between the HC and IC during dynein assembly. Such interactions might help to explain the decreased stability of dynein upon the depletion of the LIC. We have previously found that IC subunit structure can be modulated by interaction with light chain subunits (Makokha *et al*., 2002; Nyarko *et al*., 2004). Our observations also suggest that the HC does not efficiently bind to kinetochores independently, because after depletion of the IC we detect very little HC binding at the kinetochore (Figure 6, C and D). Thus, we favor a model in which the dynein IC is important for mediating the binding of dynein to kinetochores. A direct role for the IC in the targeting of cytoplasmic dynein to membranous cargoes has been reported previously (Steffen *et al*., 1997).

Despite their localization at kinetochores, the role of light chains in kinetochore dynein attachment and function is not clear. In vertebrates, there is in vitro evidence that DYNLT3, a dynein light chain related to Tctex-1, can bind to and colocalize with the checkpoint protein, Bub3 (Lo *et al*., 2007). In *Drosophila* the *Tctex-1* light chain gene is not essential (Li *et al*., 2004), and, not surprisingly, we find that RNAi depletion of the Tctex-1 subunit does not alter the localization of kinetochore dynein or Mad2 during normal mitotic progression. Whether other light chains play a role in dynein localization at kinetochores is yet to be addressed. As reported previously, the LC7 light chain is essential and mutants exhibit phenotypes throughout all mitotic phases (Bowman *et al*., 1999). This could reflect a direct role in the localization and function of dynein at kinetochores or instead could result from the loss of dynein stability.

The differential phosphorylation of dynein subunits may regulate dynein motor function at kinetochores. Our studies provide evidence that the *Drosophila* LIC is phosphorylated in vivo, consistent with previous studies in *Xenopus* and rat (Niclas *et al*., 1996; Dell *et al*., 2000; Addinall *et al*., 2001). Distinct phosphoisoforms are present in the dynein 20S complex and copurify in microtubule pellets. LIC phosphorylation may regulate specific interactions of the LIC and dynein complex. For example, in *Xenopus* and rat, the hyperphosphorylation of LIC is proposed to release cytoplasmic dynein from membranes and down-regulate vesicle transport during mitosis (Niclas *et al*., 1996; Addinall *et al*., 2001). As discussed above, our results show that LIC is required for the shedding of kinetochore dynein during the congression of chromosomes. The depletion of LIC inhibits dynein function and mitotic progression. Because phosphorylation is a major regulatory mechanism involved in the control of cell cycle progression, it will be important to determine whether phosphorylation of LIC controls the mitotic functions of dynein, including its role in checkpoint inactivation. The characterization and reagents presented here, including a *Dlic* null mutation and a functional genomic transgene that rescues the lethal phenotype, will provide a foundation for these future studies.

ACKNOWLEDGMENTS

We thank the Bardwell and Simon laboratories for help with qPCR, and we acknowledge Claudio Sunkel (Instituto de Biologia Molecular e Cellular) and Steve Henikoff (HHMI, Fred Hutchinson Cancer Research Center) for the gifts of Mad2 and CID antibody, respectively. Thanks to members of the Hays laboratory for critical reading of the manuscript. This work was completed by S.E.M. in partial fulfillment of the requirements for a Ph.D. degree (University of Minnesota) and was supported by the National Institutes of Health grant GM-044757 (to T.S.H).

REFERENCES

Addinall, S. G., Mayr, P. S., Doyle, S., Sheehan, J. K., Woodman, P. G., and Allan, V. J. (2001). Phosphorylation by cdc2-CyclinB1 kinase releases cytoplasmic dynein from membranes. J. Biol. Chem. *276*, 15939–15944.

Basto, R., Scaerou, F., Mische, S., Wojcik, E., Lefebvre, C., Gomes, R., Hays, T., and Karess, R. (2004). In vivo dynamics of the rough deal checkpoint protein during *Drosophila* mitosis. Curr. Biol. *14*, 56–61.

Bielli, A., Thornqvist, P. O., Hendrick, A. G., Finn, R., Fitzgerald, K., and McCaffrey, M. W. (2001). The small GTPase Rab4A interacts with the central region of cytoplasmic dynein light intermediate chain-1. Biochem. Biophys. Res. Commun. *281*, 1141–1153.

Bowman, A. B., Patel-King, R. S., Benashski, S. E., McCaffery, J. M., Goldstein, L. S., and King, S. M. (1999). *Drosophila* roadblock and *Chlamydomonas* LC *7*, a conserved family of dynein-associated proteins involved in axonal transport, flagellar motility, and mitosis. J. Cell Biol. *146*, 165–180.

Boylan, K., Serr, M., and Hays, T. (2000). A molecular genetic analysis of the interaction between the cytoplasmic dynein intermediate chain and the glued (dynactin) complex. Mol. Biol. Cell *11*, 3791–3803.

Boylan, K. L., and Hays, T. S. (2002). The gene for the intermediate chain subunit of cytoplasmic dynein is essential in *Drosophila*. Genetics *162*, 1211–1220.

Buffin, E., Lefebvre, C., Huang, J., Gagou, M. E., and Karess, R. E. (2005). Recruitment of Mad2 to the kinetochore requires the Rod/Zw10 complex. Curr. Biol. *15*, 856–861.

Burke, D. J., and Stukenberg, P. T. (2008). Linking kinetochore-microtubule binding to the spindle checkpoint. Dev. Cell *14*, 474–479.

Chou, T. B., Noll, E., and Perrimon, N. (1993). Autosomal P[ovoD1] dominant female-sterile insertions in *Drosophila* and their use in generating germ-line chimeras. Development *119*, 1359–1369.

Chou, T. B., and Perrimon, N. (1996). The autosomal FLP-DFS technique for generating germline mosaics in *Drosophila melanogaster*. Genetics *144*, 1673–1679.

de Cuevas, M., and Spradling, A. C. (1998). Morphogenesis of the *Drosophila* fusome and its implications for oocyte specification. Development *125*, 2781–2789.

Dell, K. R., Turck, C. W., and Vale, R. D. (2000). Mitotic phosphorylation of the dynein light intermediate chain is mediated by cdc2 kinase. Traffic *1*, 38–44.

DiBella, L. M., Sakato, M., Patel-King, R. S., Pazour, G. J., and King, S. M. (2004). The LC7 light chains of *Chlamydomonas* flagellar dyneins interact with components required for both motor assembly and regulation. Mol. Biol. Cell *15*, 4633–4646.

Dick, T., Ray, K., Salz, H. K., and Chia, W. (1996). Cytoplasmic dynein (ddlc1) mutations cause morphogenetic defects and apoptotic cell death in *Drosophila melanogaster*. Mol. Cell Biol. *16*, 1966–1977.

Echeverri, C. J., Paschal, B. M., Vaughan, K. T., and Vallee, R. B. (1996). Molecular characterization of the 50-kD subunit of dynactin reveals function for the complex in chromosome alignment and spindle organization during mitosis. J. Cell Biol. *132*, 617–633.

Faulkner, N. E., Dujardin, D. L., Tai, C. Y., Vaughan, K. T., O'Connell, C. B., Wang, Y., and Vallee, R. B. (2000). A role for the lissencephaly gene LIS1 in mitosis and cytoplasmic dynein function. Nat. Cell Biol. *2*, 784–791.

Gaetz, J., and Kapoor, T. M. (2004). Dynein/dynactin regulate metaphase spindle length by targeting depolymerizing activities to spindle poles. J. Cell Biol. *166*, 465–471.

Gaglio, T., Dionne, M. A., and Compton, D. A. (1997). Mitotic spindle poles are organized by structural and motor proteins in addition to centrosomes. J. Cell Biol. *138*, 1055–1066.

Gill, S. R., Cleveland, D. W., and Schroer, T. A. (1994). Characterization of DLC-A and DLC-B, two families of cytoplasmic dynein light chain subunits. Mol. Biol. Cell *5*, 645–654.

Golic, K. G. (1991). Site-specific recombination between homologous chromosomes in *Drosophila*. Science *252*, 958–961.

Golic, K. G., and Lindquist, S. (1989). The FLP recombinase of yeast catalyzes site-specific recombination in the *Drosophila* genome. Cell *59*, 499–509.

Gonczy, P., Pichler, S., Kirkham, M., and Hyman, A. A. (1999). Cytoplasmic dynein is required for distinct aspects of MTOC positioning, including centrosome separation, in the one cell stage *Caenorhabditis elegans* embryo. J. Cell Biol. *147*, 135–150.

Griffis, E. R., Stuurman, N., and Vale, R. D. (2007). Spindly, a novel protein essential for silencing the spindle assembly checkpoint, recruits dynein to the kinetochore. J. Cell Biol. *177*, 1005–1015.

Grissom, P. M., Vaisberg, E. A., and McIntosh, J. R. (2002). Identification of a novel light intermediate chain (D2LIC) for mammalian cytoplasmic dynein 2. Mol. Biol. Cell *13*, 817–829.

Han, K. (1996). An efficient DDAB-mediated transfection of *Drosophila* S2 cells. Nucleic Acids Res. *24*, 4362–4363.

Harada, A., Takei, Y., Kanai, Y., Tanaka, Y., Nonaka, S., and Hirokawa, N. (1998). Golgi vesiculation and lysosome dispersion in cells lacking cytoplasmic dynein. J. Cell Biol. *141*, 51–59.

Hays, T. S., Porter, M. E., McGrail, M., Grissom, P., Gosch, P., Fuller, M. T., and McIntosh, J. R. (1994). A cytoplasmic dynein motor in *Drosophila*: identification and localization during embryogenesis. J. Cell Sci. *107*, 1557–1569.

Henikoff, S., Ahmad, K., Platero, J. S., and van Steensel, B. (2000). Heterochromatic deposition of centromeric histone H3-like proteins. Proc. Natl. Acad. Sci. USA *97*, 716–721.

Hoffman, D. B., Pearson, C. G., Yen, T. J., Howell, B. J., and Salmon, E. D. (2001). Microtubule-dependent changes in assembly of microtubule motor proteins and mitotic spindle checkpoint proteins at PtK1 kinetochores. Mol. Biol. Cell *12*, 1995–2009.

Hook, P., and Vallee, R. B. (2006). The dynein family at a glance. J. Cell Sci. *119*, 4369–4371.

Howell, B. J., McEwen, B. F., Canman, J. C., Hoffman, D. B., Farrar, E. M., Rieder, C. L., and Salmon, E. D. (2001). Cytoplasmic dynein/dynactin drives kinetochore protein transport to the spindle poles and has a role in mitotic spindle checkpoint inactivation. J. Cell Biol. *155*, 1159–1172.

Hughes, S. M., Vaughan, K. T., Herskovits, J. S., and Vallee, R. B. (1995). Molecular analysis of a cytoplasmic dynein light intermediate chain reveals homology to a family of ATPases. J. Cell Sci. *108*, 17–24.

Karess, R. E., and Rubin, G. M. (1984). Analysis of P transposable element functions in *Drosophila*. Cell *38*, 135–146.

King, J. M., Hays, T. S., and Nicklas, R. B. (2000). Dynein is a transient kinetochore component whose binding is regulated by microtubule attachment, not tension. J. Cell Biol. *151*, 739–748.

King, S. J., Bonilla, M., Rodgers, M. E., and Schroer, T. A. (2002). Subunit organization in cytoplasmic dynein subcomplexes. Protein Sci. *11*, 1239–1250.

Kops, G. J., Kim, Y., Weaver, B. A., Mao, Y., McLeod, I., Yates, J. R., III, Tagava, M., and Cleveland, D. W. (2005). ZW10 links mitotic checkpoint signaling to the structural kinetochore. J. Cell Biol. *169*, 49–60.

Lee, W. L., Kaiser, M. A., and Cooper, J. A. (2005). The offloading model for dynein function: differential function of motor subunits. J. Cell Biol. *168*, 201–207.

Li, M. G., Serr, M., Newman, E. A., and Hays, T. S. (2004). The *Drosophila* tctex-1 light chain is dispensable for essential cytoplasmic dynein functions but is required during spermatid differentiation. Mol. Biol. Cell *15*, 3005–3014.

Liang, Y., Yu, W., Li, Y., Yu, L., Zhang, Q., Wang, F., Yang, Z., Du, J., Huang, Q., Yao, X., and Zhu, X. (2007). Nudel modulates kinetochore association and function of cytoplasmic dynein in M phase. Mol. Biol. Cell *18*, 2656–2666.

Lo, K. W., Kogoy, J. M., and Pfister, K. K. (2007). The DYNLT3 light chain directly links cytoplasmic dynein to a spindle checkpoint protein, Bub3. J. Biol. Chem. *282*, 11205–11212.

Logarinho, E., Bousbaa, H., Dias, J. M., Lopes, C., Amorim, I., Antunes-Martins, A., and Sunkel, C. E. (2004). Different spindle checkpoint proteins monitor microtubule attachment and tension at kinetochores in *Drosophila* cells. J. Cell Sci. *117*, 1757–1771.

Maia, A. F., Lopes, C. S., and Sunkel, C. E. (2007). BubR1 and CENP-E have antagonistic effects upon the stability of microtubule-kinetochore attachments in *Drosophila* S2 cell mitosis. Cell Cycle *6*, 1367–1378.

Maiato, H., Hergert, P. J., Moutinho-Pereira, S., Dong, Y., Vandenbeldt, K. J., Rieder, C. L., and McEwen, B. F. (2006). The ultrastructure of the kinetochore and kinetochore fiber in *Drosophila* somatic cells. Chromosoma *115*, 469–480.

Maiato, H., Rieder, C. L., and Khodjakov, A. (2004). Kinetochore-driven formation of kinetochore fibers contributes to spindle assembly during animal mitosis. J. Cell Biol. *167*, 831–840.

Makokha, M., Hare, M., Li, M., Hays, T., and Barbar, E. (2002). Interactions of cytoplasmic dynein light chains Tctex-1 and LC8 with the intermediate chain IC74. Biochemistry *41*, 4302–4311.

Malone, C. J., Misner, L., Le Bot, N., Tsai, M. C., Campbell, J. M., Ahringer, J., and White, J. G. (2003). The *C. elegans* hook protein, ZYG-12, mediates the essential attachment between the centrosome and nucleus. Cell *115*, 825–836.

McEwen, B. F., Chan, G. K., Zubrowski, B., Savoian, M. S., Sauer, M. T., and Yen, T. J. (2001). CENP-E is essential for reliable bioriented spindle attachment, but chromosome alignment can be achieved via redundant mechanisms in mammalian cells. Mol. Biol. Cell *12*, 2776–2789.

McGrail, M., and Hays, T. S. (1997). The microtubule motor cytoplasmic dynein is required for spindle orientation during germline cell divisions and oocyte differentiation in *Drosophila*. Development *124*, 2409–2419.

Merdes, A., Ramyar, K., Vechio, J. D., and Cleveland, D. W. (1996). A complex of NuMA and cytoplasmic dynein is essential for mitotic spindle assembly. Cell *87*, 447–458.

Mikami, A., Tynan, S. H., Hama, T., Luby-Phelps, K., Saito, T., Crandall, J. E., Besharse, J. C., and Vallee, R. B. (2002). Molecular structure of cytoplasmic dynein 2 and its distribution in neuronal and ciliated cells. J. Cell Sci. *115*, 4801–4808.

Musacchio, A., and Salmon, E. D. (2007). The spindle-assembly checkpoint in space and time. Nat. Rev. Mol. Cell Biol. *8*, 379–393.

Niclas, J., Allan, V. J., and Vale, R. D. (1996). Cell cycle regulation of dynein association with membranes modulates microtubule-based organelle transport. J. Cell Biol. *133*, 585–593.

Nikulina, K., Patel-King, R. S., Takebe, S., Pfister, K. K., and King, S. M. (2004). The Roadblock light chains are ubiquitous components of cytoplasmic dynein that form homo- and heterodimers. Cell Motil. Cytoskeleton *57*, 233–245.

Nyarko, A., Hare, M., Hays, T. S., and Barbar, E. (2004). The intermediate chain of cytoplasmic dynein is partially disordered and gains structure upon binding to light-chain LC8. Biochemistry *43*, 15595–15603.

O'Rourke, S. M., Dorfman, M. D., Carter, J. C., and Bowerman, B. (2007). Dynein modifiers in *C. elegans*: light chains suppress conditional heavy chain mutants. PLoS Genet. *3*, e128.

Orr, B., Bousbaa, H., and Sunkel, C. E. (2007). Mad2-independent spindle assembly checkpoint activation and controlled metaphase-anaphase transition in *Drosophila* S2 cells. Mol. Biol. Cell *18*, 850–863.

Pazour, G. J., Dickert, B. L., and Witman, G. B. (1999). The DHC1b (DHC2) isoform of cytoplasmic dynein is required for flagellar assembly. J. Cell Biol. *144*, 473–481.

Perrone, C. A., Tritschler, D., Taulman, P., Bower, R., Yoder, B. K., and Porter, M. E. (2003). A novel dynein light intermediate chain colocalizes with the retrograde motor for intraflagellar transport at sites of axoneme assembly in *Chlamydomonas* and mammalian cells. Mol. Biol. Cell *14*, 2041–2056.

Pfarr, C. M., Coue, M., Grissom, P. M., Hays, T. S., Porter, M. E., and McIntosh, J. R. (1990). Cytoplasmic dynein is localized to kinetochores during mitosis. Nature *345*, 263–265.

Pfister, K. K., Salata, M. W., Dillman, J. F., III, Vaughan, K. T., Vallee, R. B., Torre, E., and Lye, R. J. (1996). Differential expression and phosphorylation of the 74-kDa intermediate chains of cytoplasmic dynein in cultured neurons and glia. J. Biol. Chem. *271*, 1687–1694.

Pfister, K. K., Shah, P. R., Hummerich, H., Russ, A., Cotton, J., Annuar, A. A., King, S. M., and Fisher, E. M. (2006). Genetic analysis of the cytoplasmic dynein subunit families. PLoS Genet. *2*, e1.

Plamann, M., Minke, P. F., Tinsley, J. H., and Bruno, K. S. (1994). Cytoplasmic dynein and actin-related protein Arp1 are required for normal nuclear distribution in filamentous fungi. J. Cell Biol. *127*, 139–149.

Porter, M. E., Bower, R., Knott, J. A., Byrd, P., and Dentler, W. (1999). Cytoplasmic dynein heavy chain 1b is required for flagellar assembly in *Chlamydomonas*. Mol. Biol. Cell *10*, 693–712.

Purohit, A., Tynan, S. H., Vallee, R., and Doxsey, S. J. (1999). Direct interaction of pericentrin with cytoplasmic dynein light intermediate chain contributes to mitotic spindle organization. J. Cell Biol. *147*, 481–492.

Rana, A. A., Barbera, J. P., Rodriguez, T. A., Lynch, D., Hirst, E., Smith, J. C., and Beddington, R. S. (2004). Targeted deletion of the novel cytoplasmic dynein mD2LIC disrupts the embryonic organiser, formation of the body axes and specification of ventral cell fates. Development *131*, 4999–5007.

Robinson, J. T., Wojcik, E. J., Sanders, M. A., McGrail, M., and Hays, T. S. (1999). Cytoplasmic dynein is required for the nuclear attachment and migration of centrosomes during mitosis in *Drosophila*. J. Cell Biol. *146*, 597–608.

Rogers, S. L., Rogers, G. C., Sharp, D. J., and Vale, R. D. (2002). *Drosophila* EB1 is important for proper assembly, dynamics, and positioning of the mitotic spindle. J. Cell Biol. *158*, 873–884.

Savoian, M. S., Goldberg, M. L., and Rieder, C. L. (2000). The rate of poleward chromosome motion is attenuated in *Drosophila* zw10 and rod mutants. Nat. Cell Biol. *2*, 948–952.

Schafer, J. C., Haycraft, C. J., Thomas, J. H., Yoder, B. K., and Swoboda, P. (2003). XBX-1 encodes a dynein light intermediate chain required for retrograde intraflagellar transport and cilia assembly in *Caenorhabditis elegans*. Mol. Biol. Cell *14*, 2057–2070.

Spradling, A. C. (1993). Germline cysts: communes that work. Cell *72*, 649–651.

Starr, D. A., Williams, B. C., Hays, T. S., and Goldberg, M. L. (1998). ZW10 helps recruit dynactin and dynein to the kinetochore. J. Cell Biol. *142*, 763–774.

Steffen, W., Karki, S., Vaughan, K. T., Vallee, R. B., Holzbaur, E. L., Weiss, D. G., and Kuznetsov, S. A. (1997). The involvement of the intermediate chain of cytoplasmic dynein in binding the motor complex to membranous organelles of *Xenopus* oocytes. Mol. Biol. Cell *8*, 2077–2088.

Stehman, S. A., Chen, Y., McKenney, R. J., and Vallee, R. B. (2007). NudE and NudEL are required for mitotic progression and are involved in dynein recruitment to kinetochores. J. Cell Biol. *178*, 583–594.

Steuer, E. R., Wordeman, L., Schroer, T. A., and Sheetz, M. P. (1990). Localization of cytoplasmic dynein to mitotic spindles and kinetochores. Nature *345*, 266–268.

Tai, A. W., Chuang, J. Z., and Sung, C. H. (1998). Localization of Tctex-1, a cytoplasmic dynein light chain, to the Golgi apparatus and evidence for dynein complex heterogeneity. J. Biol. Chem. *273*, 19639–19649.

Tai, A. W., Chuang, J. Z., and Sung, C. H. (2001). Cytoplasmic dynein regulation by subunit heterogeneity and its role in apical transport. J. Cell Biol. *153*, 1499–1509.

Tai, C. Y., Dujardin, D. L., Faulkner, N. E., and Vallee, R. B. (2002). Role of dynein, dynactin, and CLIP-170 interactions in LIS1 kinetochore function. J. Cell Biol. *156*, 959–968.

Theodosiou, N. A., and Xu, T. (1998). Use of FLP/FRT system to study *Drosophila* development. Methods *14*, 355–365.

Tynan, S. H., Gee, M. A., and Vallee, R. B. (2000). Distinct but overlapping sites within the cytoplasmic dynein heavy chain for dimerization and for intermediate chain and light intermediate chain binding. J. Biol. Chem. *275*, 32769–32774.

Vale, R. D. (2003). The molecular motor toolbox for intracellular transport. Cell *112*, 467–480.

Vallee, R. B., Williams, J. C., Varma, D., and Barnhart, L. E. (2004). Dynein: an ancient motor protein involved in multiple modes of transport. J. Neurobiol. *58*, 189–200.

Vallee, R. B., Varma, D., and Dujardin, D. L. (2006). ZW10 function in mitotic checkpoint control, dynein targeting and membrane trafficking: is dynein the unifying theme? Cell Cycle *5*, 2447–2451.

Williams, B. C., Li, Z., Liu, S., Williams, E. V., Leung, G., Yen, T. J., and Goldberg, M. L. (2003). Zwilch, a new component of the ZW10/ROD complex required for kinetochore functions. Mol. Biol. Cell *14*, 1379–1391.

Wojcik, E., Basto, R., Serr, M., Scaerou, F., Karess, R., and Hays, T. (2001). Kinetochore dynein: its dynamics and role in the transport of the Rough deal checkpoint protein. Nat. Cell Biol. *3*, 1001–1007.

Xiang, X., Roghi, C., and Morris, N. R. (1995). Characterization and localization of the cytoplasmic dynein heavy chain in *Aspergillus nidulans*. Proc. Natl. Acad. Sci. USA *92*, 9890–9894.

Yang, Z., Tulu, U. S., Wadsworth, P., and Rieder, C. L. (2007). Kinetochore dynein is required for chromosome motion and congression independent of the spindle checkpoint. Curr. Biol. *17*, 973–980.

Yao, X., Anderson, K. L., and Cleveland, D. W. (2000). The microtubule-dependent motor centromere-associated protein E (CENP-E) is an integral component of kinetochore corona fibers that link centromeres to spindle microtubules. J. Cell Biol. *139*, 435–447.